Berreman Effect in Amorphous and Crystalline WO_3 Thin Films

B. Cláudio Trasferetti,[†] F. Paulo Rouxinol, Rogério V. Gelamo, and Mário A. Bica de Moraes*

Instituto de Física "Gleb Wataghin", Universidade Estadual de Campinas, Caixa Postal 6165, CEP: 13.083-970, Campinas, SP, Brazil

Celso U. Davanzo

Instituto de Química, Universidade Estadual de Campinas, Caixa Postal 6154, CEP: 13.083-970, Campinas, SP, Brazil

Dalva L. A. de Faria

Laboratório de Espectroscopia Molecular, Instituto de Química, Universidade de São Paulo, Caixa Postal 26077, CEP: 05513-970, São Paulo, SP, Brazil

Received: September 5, 2003; In Final Form: March 1, 2004

Thin films of tungsten oxide deposited by hot filament metal oxide deposition (HFMOD) were thermally annealed up to 800 °C and investigated by means of XRD, Raman spectroscopy, and infrared reflection−absorption spectroscopy (IRRAS). As clearly shown by the XRD and Raman spectroscopy data, the deposited films were amorphous and crystallized by thermal annealing. The monoclinic WO_3 phase was formed in all annealed samples. The IRRAS spectra were obtained using the IR beam with p-polarization and an off-normal incidence angle. In this condition, absorptions due to the longitudinal optical (LO) modes (Berreman effect) can be observed in the spectra. Absorptions due to LO modes are not detected by the standard infrared absorption spectroscopy, in which an unpolarized IR beam is used at normal incidence, and thus are not frequently reported in the literature. To analyze the experimental IRRAS spectra, the LO and TO functions were calculated from the transmission spectra of the as-deposited sample, using the Kramers−Krönig transformation and spectral simulation was carried out using the optical constants of both amorphous and crystalline WO_3. For the as-deposited sample, the LO function of the films exhibited a very prominent band at around 950 cm^{-1} which was also observed in the IRRAS spectra for all samples. For the annealed samples, this band shifted to higher wavenumbers and narrowed and a series of low-intensity bands appeared around 950 cm^{-1}, since crystalline structure changes were induced by thermal treatment. The results signal the applicability of the Berreman effect to the phase characterization of metal−supported WO_3 films.

I. Introduction

Tungsten oxide films have been the focus of extensive scientific investigations due to their prospective technological applications in electrochromic devices,[1−3] high energy density microbatteries,[4] gasochromic sensors,[5,6] and electrocatalysis.[7,8]

Although very simple in terms of stoichiometric formula, WO_3 is known to be very complex as far as structure and phase transitions are concerned.[9−15] The crystalline WO_3 phases are built from corner-sharing WO_6 octahedra bearing considerable deviations from the ideal perovskite type, the distortions corresponding to "antiferroelectric" displacements of the W atoms and mutual rotations of the oxygen octahedra. As in most of the substances with a perovskite-like structure, the type and the magnitude of the distortions are found to be dependent on the temperature and the pressure. Therefore, tungsten trioxide undergoes successive temperature- and pressure-dependent phase transitions, which are characterized by the tilting of WO_6 octahedra units and the displacement of tungsten atoms from their central octahedral positions.

In studies within this framework, Raman spectroscopy, along with X-ray diffraction, plays an important role as a WO_3 phase characterization technique. Infrared (IR) spectroscopy, however, is not a widespread phase characterization technique for WO_3 solids despite the works that were published within the spectroelectrochemical framework.[16−21] One of the advantages of using IR spectroscopy is that it can be used in the chemical characterization of amorphous oxides. As for the two other techniques, XRD cannot be used to study amorphous solids and acquiring Raman spectra of amorphous oxide samples sometimes is not very favorable since they are not good scatterers. However, Raman spectroscopy can be a valuable tool to investigate hydroxyl-related and W═O-group-related bands in tungsten oxides.[8,22,23] Particularly for the analysis of thin films, the IR technique known as infrared reflection−absorption spectroscopy (IRRAS) has proven to be very useful. Since for this technique the film is deposited onto a highly reflective surface (e.g., metallic coating on a glass substrate), the spectra are free from any possible absorption due to the substrate. Furthermore, reflection on the mirror surface produces an increase in the beam path across the film, increasing the absorption sensitivity. When obliquely incident light is used in IRRAS, longitudinal optical (LO) modes, which are not

* Corresponding author: bmoraes@ifi.unicamp.br.

[†] Present address: Departamento de Polícia Federal, Superintendência Regional no Piauí, Setor Técnico-Científico, Avenida Maranhão, 1022/N, CEP: 64.000-010, Centro, Teresina, PI, Brazil.

10.1021/jp036653u CCC: $27.50
Published on Web 07/27/2004

observed by normal incidence experiments, can be detected. Such an observation is known as a Berreman effect.[16]

In recent papers,[25−28] we have shown that the Berreman effect can be applied to the phase characterization of TiO_2 films, and we propose here that the same approach can be applied to tungsten oxide. Thus, in this paper we describe an investigation on the structural and phase changes of WO_3 films as a function of the annealing temperature using IRRAS, Raman Spectroscopy, and XRD. The films were obtained by a new deposition method developed in our laboratory, called hot filament metal oxide deposition (HFMOD) described in previous articles.[3,29,30] Briefly, a tungsten filament is heated in a rarefied oxygen atmosphere. The film is formed on a substrate positioned near the filament from volatile oxide species generated on the heated tungsten surface from reactions between oxygen and tungsten.

To understand the IRRAS spectrum of the amorphous WO_3 film, we have calculated its LO and transverse optical (TO) functions[31−34] in the mid-infrared through the Kramers−Krönig analysis of transmittance spectra.[35,36] The splitting between LO and TO maxima for a given vibrational mode is sensitive to the density of the corresponding oscillators within the solid structure.[37,38] However, for a considerable splitting to be observed, a relatively high oscillator strength is mandatory. Therefore, a significant LO−TO splitting is expected for polar-bond-related modes, such as the Si−O, Ti−O, and W−O asymmetrical stretchings.

II. Experimental Section

Film depositions were carried out by using an apparatus described in refs 3,29, and 30. In a brief description, a tungsten filament, installed in a vacuum chamber, was resistively heated by a current supply while oxygen was admitted into the chamber via an electronic mass flowmeter. The substrate−filament separation was 22 mm. A Roots pump pumped the chamber, and pressure measurements were made using a capacitance manometer. The chamber base pressure was about 2.0×10^{-2} Pa. Substrate temperatures were measured using a chromel−alumel thermocouple and filament temperatures were determined with an optical pyrometer through a chamber viewport. The thicknesses of the samples were determined using a high-resolution profilometer. Samples were deposited using a filament temperature of 1270 °C and an oxygen flow rate of 15 sccm. Platinum-coated silicon wafers and a KBr plate were used as substrates. The sample deposited on KBr was labeled WKB and was not thermally treated. Samples deposited on platinum were annealed for 1 h at 400, 600, and 800 °C and were accordingly labeled as W400, W600, and W800. One of the samples deposited on platinum was not annealed and was labeled WAD. The thicknesses of the samples were measured using a high resolution profilemeter and averaged 430 nm for all samples previously to the annealing.

Both the infrared transmission and reflection−absorption spectra were measured for all samples in a Bomen MB-101 FT-IR spectrometer equipped with a DTGS detector. The spectral range covered was 250−5000 cm^{-1}. Each spectrum was the result of coadding 64 scans collected at a 4 cm^{-1} resolution, in the transmission and external-specular-reflectance mode. For the IRRAS measurements, a variable-angle attachment (SPECAC) was used. The incidence angle was 70° off-normal, and the incident beam was p-polarized. Polarization was provided by the insertion of a grid polarizer (SPECAC) in the optical path. All reflection−absorption measurements were referenced to the bare platinum surface of a platinum-coated Si substrate, whereas the transmission ones were referenced to a bare KBr disk. All the spectra were obtained at room temperature.

For the Raman spectra acquisition, a Renishaw Raman microscope was used with excitation at 632.8 nm (He−Ne laser, Spectra Physics model 127) and beam power adjusted at 0.4 mW. The equipment is fitted with a thermoelectrically cooled CCD detector (Wright, 600 × 400 pixels) and with an Olympus metallurgical microscope.

The XRD patterns were obtained using the monochromatized Cu Kα line ($\lambda = 0.154$ nm) of a Shimadzu XRD 6000 spectrometer. The scanning was in the 2θ-range of 15°−100° with a step size of 0.02°. The identification of crystalline phases was attempted by using the Program X'Pert HighScore made by Philips.

To obtain the TO- and LO-functions, the equations

$$\text{TO-function} = \text{Im}(\tilde{\epsilon})$$

$$\text{LO-function} = \text{Im}(-1/\tilde{\epsilon})$$

were used, where $\tilde{\epsilon}$ is the complex dielectric function which can be expressed in terms of the optical constants n and k (refractive and absorption indices, respectively) by $\tilde{\epsilon} = (n + ik)^2$. Both n and k were calculated from the transmission infrared spectrum of the film deposited onto the KBr substrate, using a procedure described elsewhere.[35,37,39] In brief, k is determined directly from the spectrum using the Beer−Lambert equation.[35] From the knowledge of k and from the value of n_∞ (the refraction index of the material in the visible range, determined using the Abeles method[40]), n is calculated through the Kramers−Krönig analysis (KKA).[37] For details, see ref 41.

The simulations of reflection−absorption spectra of thin WO_3 films deposited onto a metallic substrate were carried out through the Fresnel equation for a three-phase layered system. For details on this calculation, see ref 42.

III. Results

In our previous paper,[3] in which we describe the HFMOD technique for the first time, we have observed that when keeping the filament temperature at 1320 °C and working with a range of oxygen pressure ranging from 0.8 to 2.1 Pa, the as-deposited films were constituted of amorphous stoichiometric WO_3, as revealed by XPS and XRD analysis. Therefore, we assume that the deposition conditions we use here yield similar results.

A. X-ray Diffraction. The effect of annealing on the WO_3 films is illustrated by the X-ray diffractograms of Figure 1. The thicknesses of the as-deposited films were about 430 nm, and for crystalline tungsten oxide films, this thickness would be sufficient to exhibit diffraction peaks in the 2θ-region between 10° and 100°. In the diffractogram of the as-deposited film (WAD), only the substrate Si peak and platinum peaks appear; the absence of the oxide peaks and the broad diffuse background between 10° and 40° reveal that the film is amorphous. For samples annealed at temperatures of 400 °C and above (samples W400, W600, and W800), the change of the amorphous to the crystalline phase is demonstrated by the appearance of the diffraction peaks characteristic of WO_3. The lack of the broad band between 10° and 40° in the spectrum of sample W400 suggests that the conversion of the amorphous to the crystalline phase is complete even for the annealing at 400 °C. The XRD analysis carried out using the program X'Pert HighScore allowed us to infer that samples W400, W600, and W800 were constituted by monoclinic WO_3.

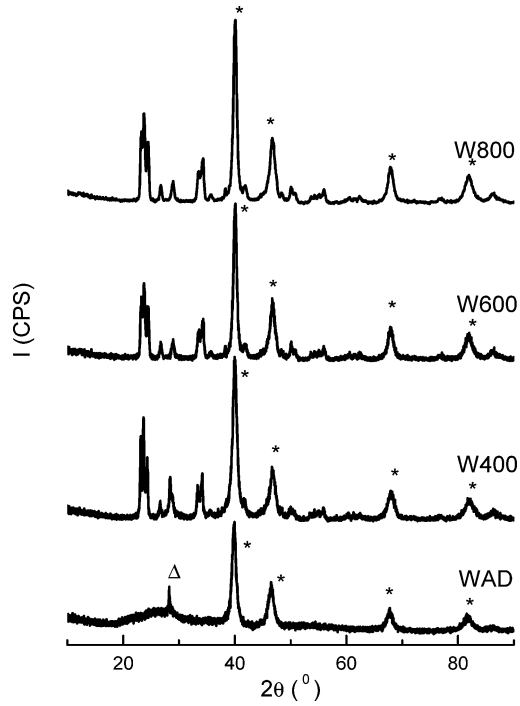

Figure 1. XRD patterns of the as-deposited (WAD) and thermally treated samples (W400, W600, and W800). Platinum peaks are specified by an asterisk, and a silicon-related peak is specified by △.

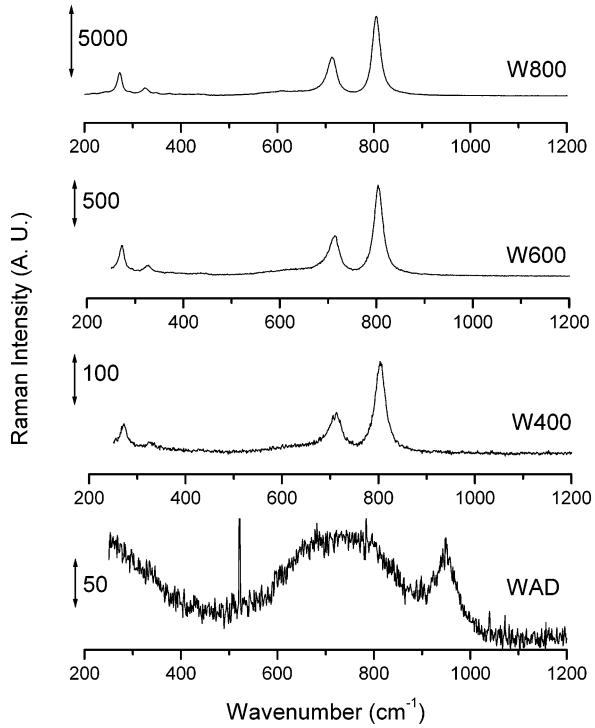

Figure 2. Raman spectra of the as-deposited (WAD) and annealed samples (W400, W600, and W800).

B. Raman Spectroscopy. Figure 2 shows the Raman spectra for the as-deposited sample and for those annealed at the temperatures of 400, 600, and 800 °C. The spectrum of the as-deposited sample shows two bands of very low intensity: a broad band centered at ∼740 cm^{-1} resulting from O−W^{6+}-O bonds and a relatively sharp one at 948 cm^{-1}, resulting from the W^{6+}═O stretching mode of terminal oxygen atoms, possibly on the surfaces of WO_3 grains and microvoid structures in the film.[22,23] The latter is characteristic of hydrated WO_3.[8] The change of the crystalline state of the samples induced by the thermal treatment implies different Raman spectra with well-defined bands at 271, 325, 713, and 805 cm^{-1}, which fall very close to the wavenumbers of the four main bands of monoclinic WO_3.[8,22,23] The bands at 271 and 325 cm^{-1} correspond to O−W−O bending modes of bridging oxygen, and the bands at 713 and 805 cm^{-1} are the corresponding stretching modes. Owing to the annealing temperature, the films dehydrate and the peak corresponding to the terminal W═O stretching mode at 948 cm^{-1} is no longer observed. It is interesting to note that there was a high intensification of the Raman signal with the increasing temperature. This may be related to an increase in the grain size of the crystallites. Consistently with the XRD data analysis, Raman analysis revealed that the crystalline phase formed was the monoclinic one and that it persisted up to the 800 °C-treated sample.

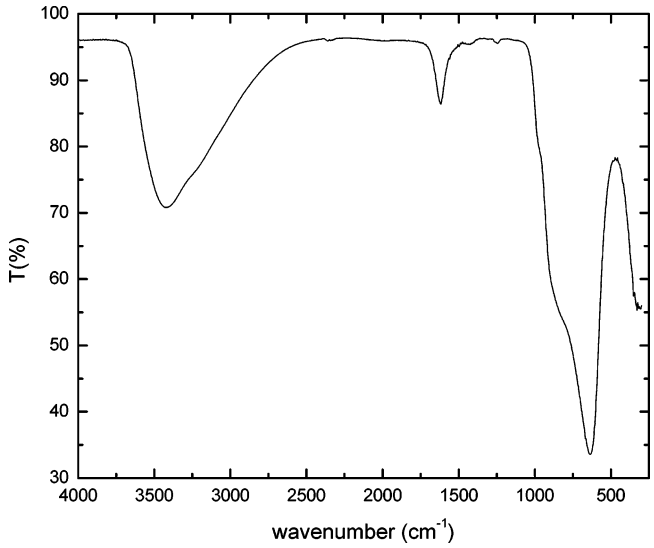

Figure 3. IR transmission spectrum for sample WKB.

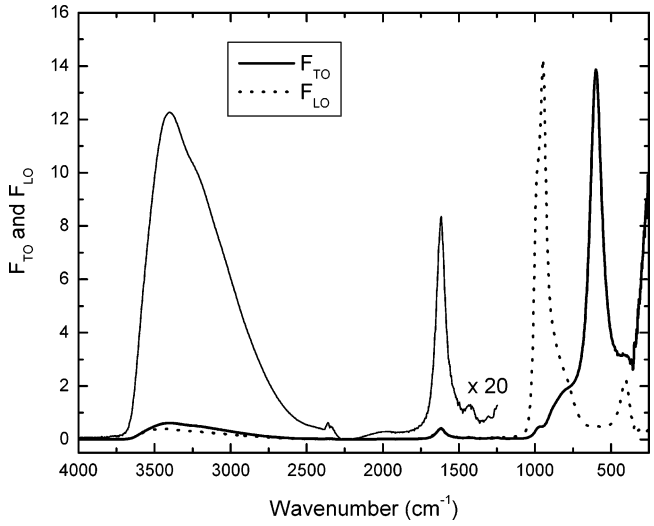

Figure 4. LO−TO functions for sample WKB. The high-frequency region of the TO function was magnified to evidence the water-related bands.

C. Infrared Spectroscopy. Figure 3 shows the transmission spectrum for sample WKB. By following the procedure briefly described in the Experimental Section (for details, see ref 25), we have calculated the LO and TO functions for this sample, which are shown in Figure 4. As far as a literature search has revealed, this is the first time that LO and TO functions for an amorphous WO_3 sample is presented. The TO function exhibits

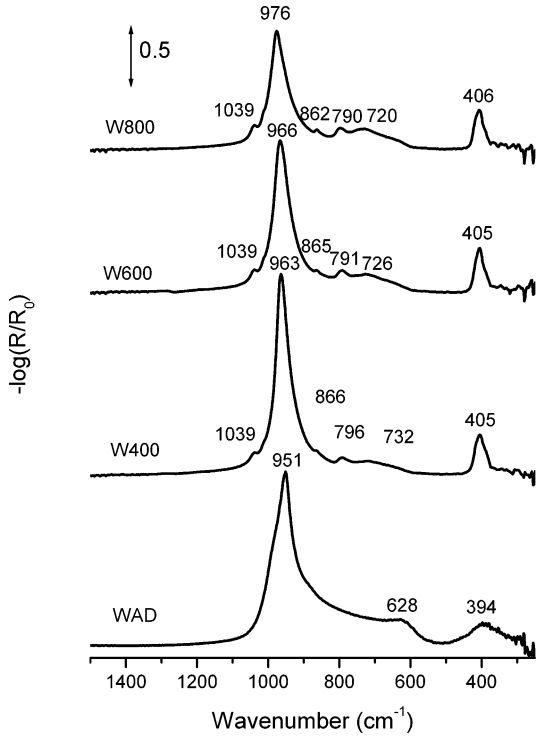

Figure 5. Infrared reflection−absorption spectra for the samples deposited onto Pt-coated silicon wafers.

a relatively sharp band with a maximum at 596 cm^{-1} with shoulders at higher and lower wavenumbers. There is also a far-infrared band, but we could not assess its maximum, since it is lower than 250 cm^{-1}, the lower limit of the wavenumber range investigated. As for the LO function, there are two main bands: the most intense one, centered at 947 cm^{-1} and exhibiting a low-wavenumber shoulder, and the less intense, at 407 cm^{-1}. Besides these W−O bond-related bands, there are also bands related to water in both the LO and TO functions at 1618 and 3400 cm^{-1}. No LO−TO splitting was observed for these bands. The band at 1618 cm^{-1} can be assigned to the deformation mode of H_2O. Its position, above the gas-phase value[43] of 1595 cm^{-1} and below that of liquid water[44] (1640 cm^{-1}), indicates the presence of H_2O molecules in a network of hydrogen bridges. The band at 3400 cm^{-1} can be assigned to the stretching of O−H bonds in H_2O. The observation of these water-related bands is consistent with the results obtained by Raman spectroscopy for the as-deposited film. We also observed a very low-intensity band at ∼1433 cm^{-1} by magnifiying the TO function in the high-frequency region of the spectrum. Knözinger and co-workers[45] have observed a band in the same frequency region that was attributed to the OHO bending vibration of molybdenum hydrates. Analogically, the band observed can be related to the presence of hydrates within the bulk of our as-deposited WO_3 films.

For the annealed samples, the method for retrieving the optical constants from transmission spectra could not be used because KBr cannot withstand thermal treatments. To overcome this problem, the optical constants and the LO and TO functions retrieved from the quasi-normal reflection spectrum reported by Gabrusenoks and co-workers[46] for a monoclinic WO_3 single crystal will be used.

Figure 5 shows the reflection−absorption spectra for the samples deposited onto Pt-coated silicon wafers. To analyze them, we have simulated reflection−absorption spectra for both amorphous and crystalline films using a three-phase model derived from the optical theory.[42] The optical constants used

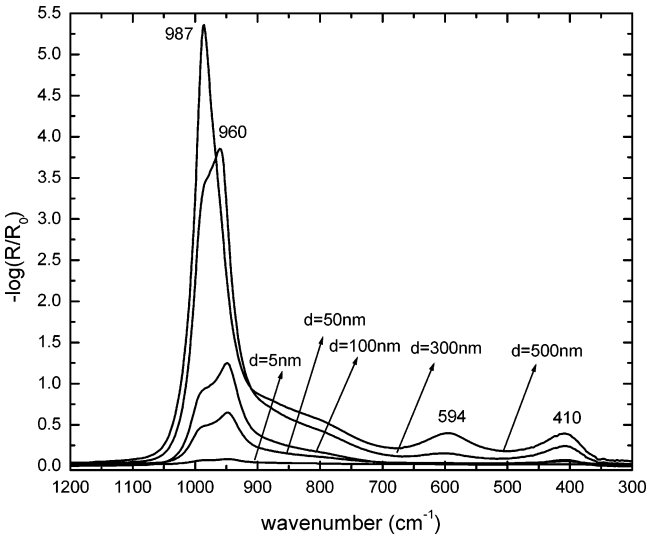

Figure 6. Simulated reflection−absorption spectra of a WO_3 film deposited onto platinum with an incident angle of 70° and p-polarized light (d stands for film thickness). The optical constants for the films were those calculated for sample WKB.

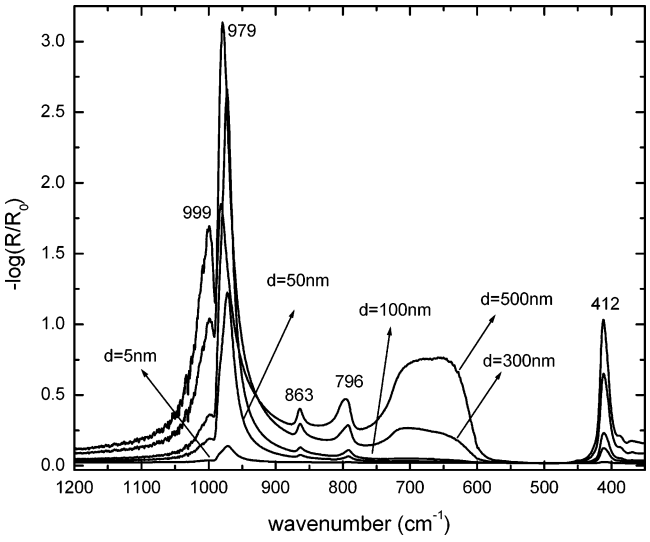

Figure 7. Simulated reflection−absorption spectra of WO_3 films deposited onto platinum with an incident angle of 70° and p-polarized light. The optical constants for the films were derived from quasi-normal reflection data of a monoclinic WO_3 single crystal reported by Gabrusenoks and co-workers.[46]

for the simulation of the reflection−absorption spectra of amorphous samples (shown in Figure 6) were those determined for sample WKB. For the spectral simulation of crystalline samples (shown in Figure 7), we have used the data provided by Gabrusenoks and co-workers.[46]

The spectra shown in Figure 6 are important to analyze the IRRAS spectra of the as-deposited sample (WAD) shown in Figure 5, which, according to the XRD and Raman analyses, is composed of an amorphous hydrated tungsten oxide. The most prominent band of the IRRAS spectrum of this sample lies at 951 cm^{-1}, which is very close to the LO band of Figure 4 and to the band observed in the simulated spectra in Figure 6, with a tail toward lower wavernumbers. It also has two broad and low-intensity bands centered at 628 and 394 cm^{-1}. The former may have resulted from the superimposition of the LO and TO modes. The latter is centered at a wavenumber that is close to the less intense LO band of Figure 4. However, unlike this band, it is very broad. Since band-narrowing is often related to

crystallization processes, we have compared the XRD diffractograms of samples WAD and WKB (not shown) and there was no oxide film-related differences, which is consistent with an amorphism of both samples. It seems to us that although both films are amorphous, there are subtle structural differences between samples WAD and WKB, which may have been caused by a substrate-driven process that occurred during or after deposition. Though subtle, these differences may be strong enough to cause differences in the IR spectra. In light of Ovchinnikov and Wight's work on inhomogeneously broadened LO and TO bands of amorphous solids,[47] such differences can be caused by the size and/or shape of the cells of the disordered lattice of films deposited in different substrates.

Turning to the effects of the annealing treatment, Figure 5 illustrates the IRRAS spectra of the crystallized samples. As before, an analysis of such spectra, based on the simulated spectra shown in Figure 7, is of interest. From Figure 5, the main band observed at 951 cm^{-1} for the WAD sample blue-shifts up to 976 cm^{-1} for sample W800 and loses its low-frequency tail to gain a few low-intensity bands at ~725, ~795, ~865, and ~1039 cm^{-1}. Most of these bands correspond to those seen in either the TO or LO function of the single crystal:[46] the band at ~725 cm^{-1} to a TO mode and those at ~795, ~865 to LO modes. They also correspond to the bands observed in Figure 7 for the simulated spectra. The only band that does not have a counterpart in the single crystal's LO function is the one observed at ~1039 cm^{-1}. A band at ~998 cm^{-1} can be seen in the single crystal's LO function, but it does not seen to be related with that at ~1039 cm^{-1}, since they are too far apart (~41 cm^{-1}). We speculate that the band at 1039 cm^{-1} can be tentatively attributed to bulk W═O moieties. Chan and co-workers[16] have observed a band at 1015 cm^{-1} for samples of WO_3 films on powdered titania, which they assigned to W═O. But after allowing these samples to be in contact with moisture, this band moves to ~960 cm^{-1}, which suggests that it is environment-sensitive. In our case, since the films were kept in air, we assume that they bear W═O bonds that are far from the WO^3/air interface and close to the WO_3/Pt interface, which suggests that the appearance of this band is related to the metal surface selection rule.

Another effect of the annealing is both the blue-shift to 405 cm^{-1} and the narrowing of the broad band at 394 cm^{-1} of sample WAD. The LO function for the single crystal lies at 412 cm^{-1}. The good agreement between the band positions of our spectra with those observed by Gabrusenoks and co-workers[46] allows us to infer that the crystalline phase formed is indeed the monoclinic one. The same inference was made from XRD and Raman spectroscopy results.

IV. Conclusions

We have investigated the effects of an annealing treatment on WO_3 thin films deposited by HFMOD by means of XRD, Raman, and infrared reflection−absorption spectroscopies. Both Raman and XRD are well-established phase characterization techniques and were used to support the interpretation of the spectra obtained by the IRRAS technique, which is not commonly applied to the phase characterization of WO_3. Several spectral occurrences in the annealed samples, such as the appearance of new IR bands and the narrowing of the main LO bands at ~950 cm^{-1}, signaled the crystallization process, which indicates that the Berreman effect is applicable to the phase characterization of WO_3.

Acknowledgment. The Fundação de Amparo à Pesquisa do Estado de São Paulo (Grant No. 02/07482-6), CAPES, and CNPq are thanked for financial support. We also thank Dr. Gabrusenoks, from the University of Latvia, for providing us with the LO and TO functions of a monoclinic WO_3 single crystal and Dr. Heloise O. Pastore, Dr. Lisandro P. Cardoso, and Mr. Adenilson O. dos Santos for helping with the XRD analysis. The help of Mr. José Godoy Filho with the annealing of the samples and that of Mr. Carlos Salles Lambert for providing platinum-coated silicon wafers is greatly acknowledged.

References and Notes

(1) Granqvist, C. G. Electrochromism and Electrochromic Devices. In *The CRC Handbook of Solid State Electrochemistry*; Gellings, P. J., Bouwmesster, H. J. M., Eds.; CRC Press: 1997; Chapter 16.
(2) Bange, K. *Sol. Energy Mater. Sol. Cells* **1999**, *58*, 1.
(3) Scarminio, J.; Bica de Moraes, M. A.; Dias, R. C. E.; Rouxinol, F. P.; Durrant, S. F. *Electrochem. Solid State Lett.* **2003**, *6*, H9.
(4) Varella, H.; Huguenin, F.; Malta, M.; Torresi, R. M. *Quim. Nova* **2002**, *25*, 287.
(5) Lee, S.-H.; Cheong, H. M.; Liu, P.; Smith, D.; Tracy, C. E.; Mascarenhas, A.; Pitts, J. R.; Deb, S. K. *J. Appl. Phys.* **2000**, *88*, 3076.
(6) Solis, J. L.; Saukko, S.; Kish, L.; Granqvist, C. G.; Lantto, V. *Thin Solid Films* **2001**, *391*, 255.
(7) Roland, J. F.; Anson, F. C. *J. Electroanal. Chem.* **1992**, *336*, 245.
(8) Habazaki, H.; Hayashi, Y.; Konno, H. *Electrochim. Acta* **2002**, *47*, 4181.
(9) Salje, E.; Viswanathan, K. *Acta Crystallogr.* **1975**, *A31*, 356.
(10) Salje, E. *Acta Crystallogr.* **1975**, *A31*, 360.
(11) Salje, E. *Acta Crystallogr.* **1977**, *B33*, 574.
(12) Hayashi, S.; Sugano, H.; Arai, H.; Yamamoto, K. *J. Phys. Soc. Jpn.* **1992**, *61*, 916.
(13) Souza Filho, A. G.; Freire, V. N.; Sasaki, J. M.; Mendes Filho, J.; Julião, J. F.; Gomes, U. U. *J. Raman Spectrosc.* **2000**, *31*, 695.
(14) Souza Filho, A. G.; Freire, P. T. C.; Pilla, O.; Ayala, A. P.; Mendes Filho, J.; Melo, F. E. A.; Freire, V. N.; Lemos, V. *Phys. Rev. B* **2000**, *62*, 3699.
(15) Souza Filho, A. G.; Mendes Filho, J.; Freire, V. N.; Ayala, A. P.; Sasaki, J. M.; Freire, P. T. C.; Melo, F. E. A.; Julião, J. F.; Gomes, U. U. *J. Raman Spectrosc.* **2001**, *32*, 695.
(16) Chan, S. S.; Wachs, I. E.; Murrell, L. L.; Wang, L.; Hall, W. K. *J. Phys. Chem.* **1984**, *88*, 5831.
(17) Yoshiike, N.; Mizuno, Y.; Kondo, S. *J. Electrochem. Soc.* **1984**, *131*, 2634.
(18) Daniel, M. F.; Desbat, B.; Lassègues, J.-C.; Gerand, B.; Figlarz, M. *J. Solid State Chem.* **1987**, *67*, 235.
(19) Daniel, M. F.; Desbat, B.; Lassègues, J.-C.; Garie, R. *J. Solid State Chem.* **1988**, *73*, 127.
(20) Badilescu, S.; Ashrit, P. V.; Girouard, F. E.; Truong, V.-V. *J. Electrochem. Soc.* **1989**, *136*, 3599.
(21) Paul, J.-L.; Lassègues, J.-C. *J. Solid State Chem.* **1993**, *106*, 357.
(22) Lee, S.-H.; Cheong, H. M.; Liu, P.; Smith, D.; Tracy, C. E.; Mascarenhas, A.; Pitts, J. R.; Deb, S. K. *Electrochim. Acta* **2001**, *46*, 1995.
(23) Lee, S.-H.; Cheong, H. M.; Liu, P.; Smith, D.; Tracy, C. E.; Mascarenhas, A.; Pitts, J. R.; Deb, S. K. *J. Appl. Phys.* **2000**, *48*, 3076.
(24) Berreman, D. W. *Phys. Rev.* **1963**, *130*, 2193.
(25) Trasferetti, B. C.; Davanzo, C. U.; da Cruz, N. C.; Bica de Moraes, M. A. *Appl. Spectrosc.* **2000**, *54*, 687.
(26) Trasferetti, B. C.; Davanzo, C. U.; Zoppi, R. A.; da Cruz, N. C.; de Moraes, M. A. B. *Phys. Rev. B* **2001**, *64*, 125404.
(27) Trasferetti, B. C.; Davanzo, C. U.; Zoppi, R. A. *Electrochem. Commun.* **2002**, *4*, 301.
(28) Zoppi, R. A., Trasferetti, B. C.; Davanzo, C. U. *J. Electroanal. Chem.* **2003**, *544*, 47.
(29) Bica de Moraes, M. A.; Trasferetti, B. C.; Rouxinol, F. P.; Landers, R.; Durrant, S. F.; Scarmínio, J.; Urbano, A. *Chem. Mater.* **2004**, *16*, 513.
(30) Rouxinol, F. P.; Trasferetti, B. C.; Landers, R.; Bica de Moraes, M. A. *J. Braz. Chem Soc.* **2004**, *15*, 324.
(31) Kittel, C. *Introduction to Solid State Physics*, 7th ed.; John Wiley & Sons: New York, 1996.
(32) Blakemore, J. S. *Solid State Physics*, 2nd ed.; Cambridge Universtiy Press: Cambridge, 1995.
(33) Ten, Y.-S.; Wong, J. S. *J. Phys. Chem.* **1989**, *93*, 7208.
(34) Harbecke, B.; Heinz, B.; Grosse, P. *Appl. Phys. A* **1985**, *38*, 263.
(35) Hawranek, J. P.; Jones, R. N. *Spectrochim. Acta* **1976**, *32*, 99.
(36) Yamamoto, K.; Ishida, H. *Vib. Spectrosc.* **1994**, *8*, 1.
(37) Trasferetti, B. C.; Davanzo, C. U.; Bica de Moraes, M. A. *J. Phys. Chem B* **2003**, *107*, 10699.
(38) Jones, L. H.; Swanson, B. I. *J. Phys. Chem.* **1991**, *95*, 2701.
(39) Trasferetti, B. C.; Davanzo, C. U.; Bica de Moraes, M. A. *Macromolecules* **2004**, *37*, 459.

(40) Heavens, O. S. *Phys. Thin Films* **1964**, *2*, 120.

(41) For the case described here, the reflective index *n* can be calculated from the absorption index by the following Kramers−Krönig equation:[35]

$$n(\nu') = n_\infty + \frac{2}{\pi} p \int_0^\infty \frac{\nu k(\nu')}{(\nu^2 - \nu'^2)} d\nu$$

where n_∞ can be taken as the refractive index in the visible range, ν is the wavenumber, and the symbol *p* refers to the principal part of the integral. As for the extrapolation required by the above equation, absorption indices obtained from the first and last points of the measured spectrum file were assumed constant.[36]

(42) The reflection amplitude *r* for the system of a film layer on a substrate can be written as a function of Fresnel reflection coefficients for each interface by applying the matrix method to a three-phase layered system. The matrix method was developed by Abèles and has been successfully employed in the modelation of optical properties of multilayered systems [Anki, M. M. T.; Lefez, B. *Appl. Opt.* **1996**, *35*, 1399]. The result of such a procedure is the following equation for the reflection amplitude of a three-phase system: $r = (r_{01} + r_{12}e^{2i\delta\zeta_1})/(1 + r_{01}r_{12}e^{2i\delta\zeta_1})$, where $\delta = 2\pi\nu d$ is the "reduced" film thickness. The phase factor $e^{2i\delta\zeta}$ accounts for the phase lag and attenuation of the beam after traversing the film. The Fresnel reflection coefficients for each interface r_{01} and r_{12} are defined as the following: $r_{01} = (\zeta_0 - \zeta_1)/(\zeta_0 + \zeta_1)$ and $r_{12} = (\zeta_1 - \zeta_2)/(\zeta_1 + \zeta_2)$. Although it has no physical meaning,[33] the parameter ζ is defined for convenience, in the light of the Snell's law of refraction, as $\zeta_j = (\tilde{n}_j \cos \theta_j)/\tilde{n}_j^2 = (\tilde{n}_j^2 - n1\ sen2\ \theta_0)^{1/2}/n_j^2$ for p-polarization, where θ_j is the incidence angle for phase 0 and the refraction angle for phases 1 and 2 and *j* is the phase index. The reflectance *R* of the system is then given by $|r|^2$.

(43) Morrow, B. A. In *Studies in Surface Science*; Fierro, J. L., Ed.; Elsevier: Amsterdam, 1990; Vol. 57, p 161.

(44) Bertie J. E.; Lan, Z. *Appl. Spectrosc.* **1996**, *50*, 1047.

(45) Mestl, G.; Srinivasan, T. K. K.; Hnözinger, H. *Langmuir* **1995**, *11*, 3795.

(46) Gabrusenoks, J.; Veispals, A.; von Czarnowski, A.; Meiwes-Broer, K.-H. *Electrochim. Acta* **2001**, *46*, 1921.

(47) Ovchinnikov, M. A.; Wight, C. A. *J. Chem Phys.* **1995**, *102*, 67.